The following supplement accompanies the article

'Whale wave': shifting strategies structure the complex use of critical fjord habitat by humpbacks

Eric M. Keen*, Janie Wray, Hermann Meuter, Kim-Ly Thompson, Jay P. Barlow, Chris R. Picard

*Corresponding author: ekeen@ucsd.edu

Marine Ecology Progress Series 567: 211–233 (2017)

SUPPLEMENT

Echosounder data processing and analysis aboard *RV Bangarang*

INTRODUCTION

This document outlines the steps taken in the preparation of echosounder data collected aboard the *RV Bangarang* for use in analyses of whale-prey interactions in the Kitimat Fjord System, northern British Columbia. All of these steps take place within open-source software including Visual Basic, ImageJ, Fhred, TextWrangler and R (R Core Team 2013), with routines written by EMK. Visual Basic code is available on EMK's research website, http://www.rvbangarang.org, and scripts of R and ImageJ code are available upon request.

Instrumentation

Aboard the *Bangarang*, hydroacoustic data were recorded along survey tracklines with a down-sounding *Syqwest Hydrobox* echosounder (33 and 200 kHz dual-frequency) to obtain a profile map of the depth, distribution, and patchiness of backscatter down to 300m.

The *Hydrobox* performs some preliminary processing before making data available to users. This includes the implementation of a 20logR time-varied gain and the conversion of acoustic backscatter into color pixels based on gain and threshold parameters set by the user. These parameters are locked; they do not change in response to seafloor depth or overall noise levels. Each transmission is reported in the form of 200 pixels representing backscatter from the sea surface to 300m depth, such that each pixel is a bin representing 1.5 vertical meters of water. Pixels are given as integers, ranging from 0 to 255.

The use of similar low-cost echosounders has been common in studies of cetacean and seabird foraging strategy (e.g., Dolphin 1988; Piatt 1987, 1990; Burger & Piatt 1990; Piatt & Methven 1992; O'Driscoll 1998; Benoit-Bird et al. 2001; Benoit-Bird & Au 2003). Because of the *Hydrobox*'s in-house processing, the data cannot be analyzed or described in the standard terminology of scientific echosounders as outlined in MacLennan et al. (2002). As it is not possible to conform our data to conventional units and definitions, we were careful to develop backscatter metrics that were similar to but clearly different from the standard in both unit and name.

The Bangaranag's Hydrobox transmitted at 600 Watts. Each frequency transducer was housed within the same hydrodynamic moulding. Each frequency was transmitted at a rate of 1 Hz. The frequencies were offset from each other by 0.5 sec. Gain settings within Hydrobox software were set to 27 dB for 33 kHz

and 60 dB for 200 kHz. Beam widths were 18 degree for 33 kHz and 10 degree for 200 kHz. Within Hydrobox software, the detection threshold was set to 0 for both frequencies, and a sound speed 1500 m/s was used.

The transducer body was mounted 0.5m deep (within the range of depths in Rowe 1993, Yule 2000, Benoit-Bird et al., 2001), deployed at the most stable point on the vessel at the port transom by a stainless steel pipe that was secured to the vessel's swimbridge. When not in use the transducer swings up on a hinge for safe stowage. The transducer's signal was passed via weather-proof cable to a serial hub within the vessel's dinette, then on to the data entry laptop at the helm. On this laptop the echosounder data were saved and displayed in real-time. The echosounder was powered by the ship's dedicated research battery, which was isolated from house and engine battery circuits, to eliminate electrical interference.

Frequency choice

The backscatter properties of an organism can be frequency-dependent, the details of which are primarily a function of the organism's overall size and its material properties (Romaine et al. 2002). Echograms from 38kHz sounds or lower detect mainly air-bladdered fish (Cochrane et al. 2000) or physonectid siphonophores (Farquhar, 1971; Andersen and Zahuranec, 1977). Fish with air-filled swim-bladders cause backscatter in a wide-range of frequencies, from 12 kHz to above 200 kHz (Foote 1980). Herring and young hake are the principal species associated with scattering layers in BC mainland inlets (Bary 1966, Sato et al. 2013).

Unlike air-bladdered fish, zooplankton that are iso-osmotic and only centimeters in size have much higher frequency dependence (Stanton et al. 1996, Kang et al., 2002). Many studies have used a 200kHz echosounder for detecting euphausiid swarms (e.g., Coyle and Cooney 1992, Rowe 1993, Cochrane et al., 2000, Benoit-Bird et al. 2001, Romaine et al. 2002, Sato et al. 2013).

A 38kHz and 200kHz dual-beam setup is among the most common in surveys for both fish and euphausiids (e.g., Coyle and Cooney 1992, Wiebe et al. 1997). A 38kHz transducer was not available for my system so the closest available frequency was used, 33 kHz.

Processing summary

Raw output from the Hydrobox software was converted to ASCII and timestamp-matched to visuals data. Systematic transect effort and focal follows were extracted from each day of acoustic data. GPS-stamps were used to account for variable vessel speed by pooling pings into bins representing 6m of trackline, such that each pixel value in a section of echosounder data represented a volume of water approximately 6 m x 6 m x 1.5 vertical meters.

Seafloor detections were verified by visual review and corrected using hydrographic data. Backscatter within 6m of the surface and seafloor were removed. Each day's backscatter was visually reviewed for manual removal of regions of noise caused by engine cavitation or depth sounders from passing ships. All pixel values below a chosen "biological noise floor" were then removed.

Each frequency was then inspected visually, and filters were applied that removed backscatter that did not seem attributable to potential humpback prey, which we limited for our purposes to schooling "forage" fish and euphausiids. As a simplistic kind of "frequency differencing" technique, 200 kHz backscatter that overlapped with 33 kHz backscatter was removed such that the former represented krill-like backscatter and the latter represented schooling-fish-like backscatter. These scrutinization steps were verified using deepwater imaging and zooplankton tows.

BASIC FORMATTING

The raw data provided by *Hydrobox* software has two types of NMEA strings: a pixel row (one row for each frequency) and a context row (depth, lat, long, speed, heading, etc.) These strings were saved in a single playback file in a format that requires conversion to hexadecimal characters then to ASCII.

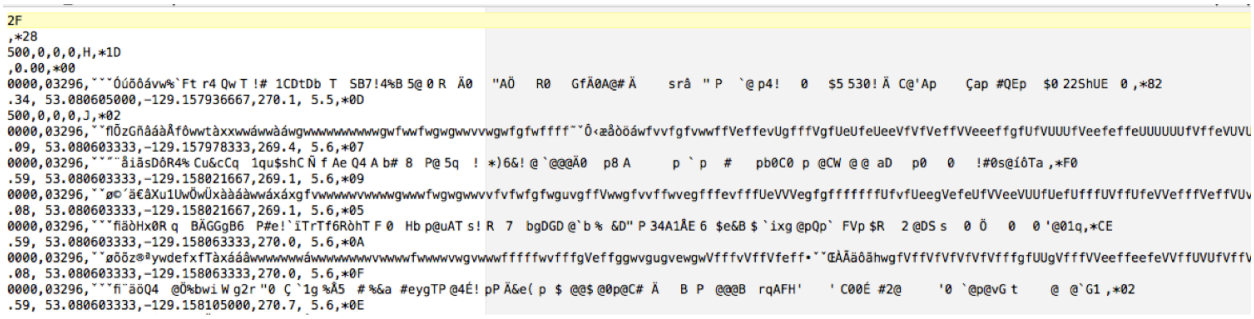

Figure S1. Screenshot of raw data output from the echosounder, in .odc format, opened in TextWrangler.

The first step is converting the file to pure hexadecimal format then breaking it into lines of text. The former is done in the open-source software Frhed and the latter is done with a custom routine written in Visual Basic.

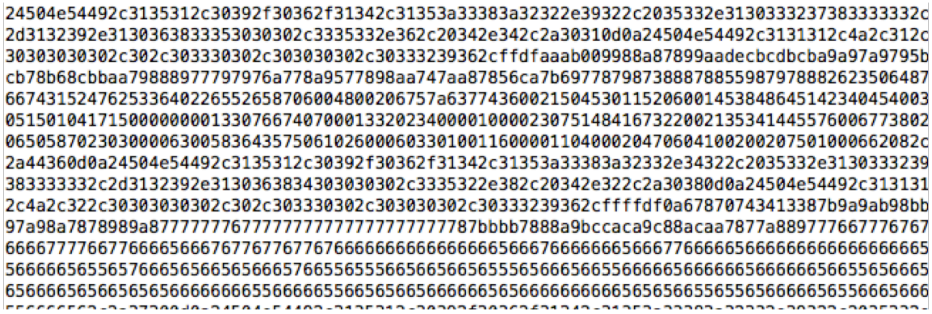

Figure S2. Screenshot of conversion of raw data to hexadecimal format, saved as a .txt file.

Figure S3. Hexadecimal data broken into lines, saved as a .txt file.

The remaining processing steps are conducted in R. Lined text files of hexadecimal characters are translated into ASCII using an ASCII conversion table. The ASCII translation is output to comma-separated text files.

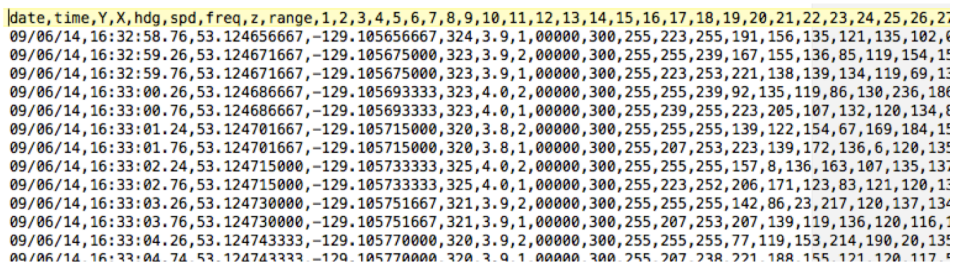

Figure S4. Screenshot of conversion to ASCII format, saved as a .csv file, visualized in Text Wrangler:

Each line of these text files is then assigned visual effort designations using timestamp-matching from the day's RUB output file. Effort-synched comma-separated files for each frequency (33kHz and 200kHz) of each date of field effort are generated and stored.

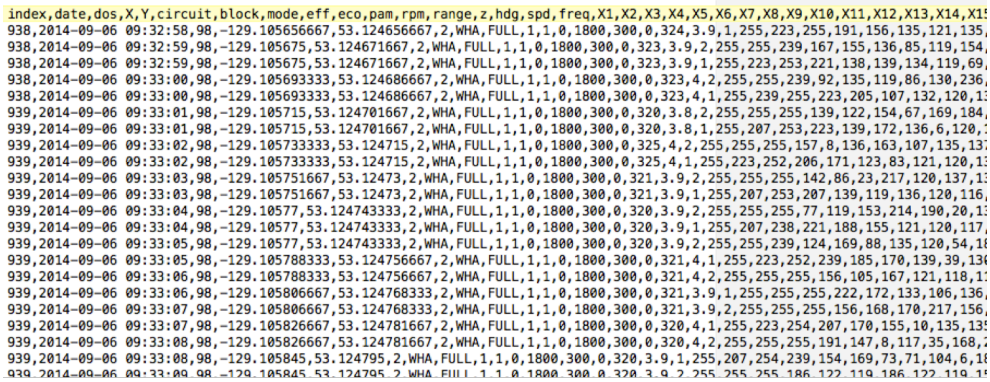

Figure S5. Screenshot of echodata with assigned survey effort data:

The echosounder software stores long recording sessions in small contiguous files of 1 MB file size. As the final step in basic formatting, all files from a single day are combined into a single file. In the same R routine EMK also standardized depth output (which is stored with variable significant figures in the raw echosounder output, depending on depth). The full-day's echo file is then visualized for quality control. Because about 55,000 pings are recorded in the average field day, the full-day files are quite large (10s of MBs).

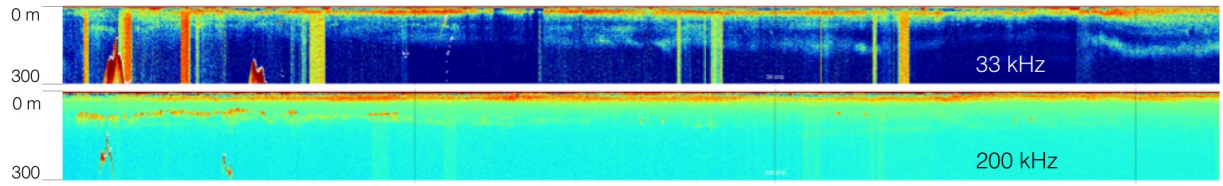

Figure S6. Example of echogram of unreduced data from a single day, 11 August 2014. Top row is 33 kHz output, bottom row is 200 kHz. Color palette is same as that used in Hydrobox echogram display software. Automatically detected seafloor is highlighted in white.

DATA REDUCTION

Subset to transects and focal follows

Using the effort codes now associated with the data, pings corresponding to periods of transect effort and focal follows are isolated and saved separately. For focal follow echograms sighting and survey information were also included as a reference. As an aid in the interpretation and processing of focal follow echograms, maps of vessel tracks during focal follows are also produced.

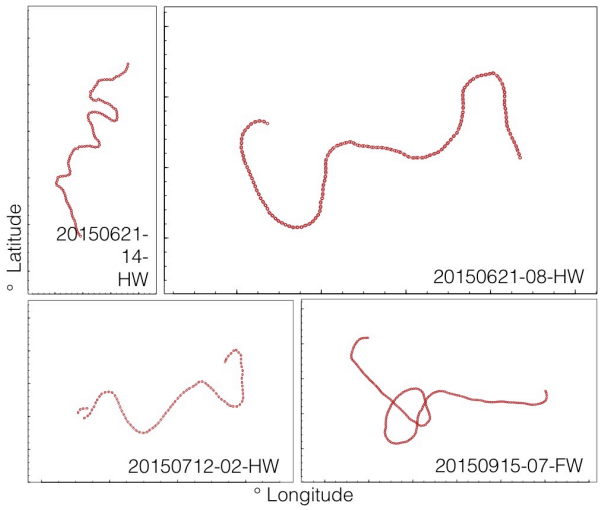

Figure S7. Example maps of focal follow tracks.

Georectify

To ensure that changes in vessel speed did not falsely represent the extent of backscatter along a trackline, echo data are "georectified" by averaging pings into bins of equal lateral distance of approximately 6m according to their GPS-stamps. The result is reduced backscatter whose pixels represent a volume of the water 6m x 6m wide x 1.5m deep (54 m^3), each calculated from the average of 1 to 10 horizontal raw pixels depending on vessel speed. Georectification is performed on both transect and focal follow data. At our average transect speed (4.5 knots, 2.3 m s^{-1}), 2 to 3 pixels are averaged together to yield a single pixel value in the georectified file. At focal follow speed, which is highly variable but a safe average is 2 knots or approximately 1 m s^{-1}), 5 to 7 pixels are averaged together for a single horizontal bin.

```
index,date,dos,X,Y,circuit,block,mode,eff,eco,pam,rpm,range,z,hdg,spd,freq,X1,X2,X3,X4,X5,X6,X7,
146,2014-09-06 07:44:40,98,-129.160175,53.080631667,2,WHA,FULL,2,0,0,1800,300,NA,294,5.2,1,255,2
147,2014-09-06 07:44:46,98,-129.160366667,53.08071,2,WHA,FULL,2,1,0,1800,300,NA,314,4.8,1,255,25
148,2014-09-06 07:44:52,98,-129.160496667,53.080811667,2,WHA,FULL,2,1,0,1800,300,NA,332,4.3,1,25
149,2014-09-06 07:45:01,98,-129.160555,53.080973333,2,WHA,FULL,2,1,0,1800,300,NA,NA,3.7,1,255,25
149,2014-09-06 07:45:10,98,-129.160496667,53.081111667,2,WHA,FULL,2,1,0,1800,300,NA,NA,3.4,1,25
150,2014-09-06 07:45:19,98,-129.160393333,53.081236667,2,WHA,FULL,2,1,0,1800,300,NA,NA,3.5,1,25
151,2014-09-06 07:45:28,98,-129.160251667,53.081346667,2,WHA,FULL,2,1,0,1800,300,NA,NA,3.3,1,25
152,2014-09-06 07:45:37,98,-129.16009,53.081435,2,WHA,FULL,2,1,0,1800,300,NA,NA,3.2,1,255,255,25
153,2014-09-06 07:45:46,98,-129.15989,53.0815,2,WHA,FULL,2,1,0,1800,300,NA,NA,3.3,1,255,255,251,
154,2014-09-06 07:45:58,98,-129.159613333,53.081561667,2,WHA,FULL,2,1,0,1800,300,NA,NA,3.3,1,25
155,2014-09-06 07:46:10,98,-129.159333333,53.08162,2,WHA,FULL,2,1,0,1800,300,NA,NA,3.3,1,255,25
157,2014-09-06 07:46:22,98,-129.159043333,53.081673333,2,WHA,FULL,2,1,0,1800,300,NA,NA,3.3,1,25
158,2014-09-06 07:46:34,98,-129.158746667,53.081711667,2,WHA,FULL,1,1,0,1800,300,NA,NA,3.2,1,25
159,2014-09-06 07:46:46,98,-129.158445,53.08172,2,WHA,FULL,1,1,0,1800,300,NA,NA,3.3,1,255,255,25
160,2014-09-06 07:46:58,98,-129.158161667,53.081763333,2,WHA,FULL,1,1,0,1800,300,NA,NA,3.3,1,25
161,2014-09-06 07:47:10,98,-129.157875,53.081818333,2,WHA,FULL,1,1,0,1800,300,NA,NA,3.3,1,255,25
164,2014-09-06 07:47:22,98,-129.157591667,53.081873333,2,WHA,FULL,1,1,0,1800,300,NA,NA,3.3,1,25
```

Figure S8. Example of georectified transect data; every row represents approximately the same horizontal distance.

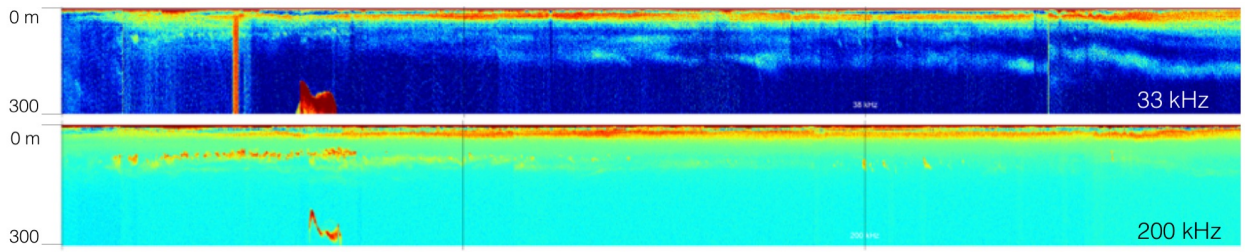

Figure S9. Echogram of georectified backscatter from 11 August 2014. Top row is 33 kHz output, bottom row is 200 kHz. Color palette is same as that used in Hydrobox echogram display software.

NOISE PROCESSING

Automated seafloor correction

As a first step in ridding data of non-biological backscatter, seafloor echoes are removed. With every ping the echosounder stores an estimate of the seafloor depth, but these estimates differ slightly between frequencies and can be "tricked" by engine cavitation or inordinately thick prey layers. Moreover, the echosounder does not estimate depth below the prescribed depth range of 300m, but an accurate local depth was needed for habitat use and prey patch analyses.

To ground-truth, correct and gap-fill the echosounder's seafloor readings, they are compared to a publicly available 3-arc-second bathymetric dataset (NOAA 2013). Because the low-frequency can reflect the seafloor more accurately at greater depths, every high-frequency seafloor reading is replaced with that of the low-frequency ping that is closest in time. Then, for each ping regardless of frequency, the perceived seafloor is GPS-matched to the closest NOAA datum using the Vincenty method of the great-sphere distance algorithm (function "distance" in R package "swfscMisc" by Eric Archer). Only matches within a maximum distance (0.005 degrees latitude) are accepted, so that distant NOAA data would not be mistakenly used. Because our echosounder data have much greater resolution than the 3-arc-second dataset, the NOAA data are interpolated between adjacent readings to make seafloor slopes less jagged.

The NOAA datum is kept as the correct depth 1) if the NOAA data show that the vessel was in greater than 300m of water, or 2) if the echosounder's reading reads “NA”. The echosounder reading was kept 1) if both the NOAA match and echosounder reading reported a depth less than 300m, and 2) when no NOAA datum occurred within 0.005 degrees of the vessel at the time of the ping. The seafloor correction routine outputs a graph that displays the decisions made datum by datum. Depth-corrected data files are output along with an echogram that displays the corrected seafloor superimposed. These same seafloor correction processes are also applied to focal follow echo data.

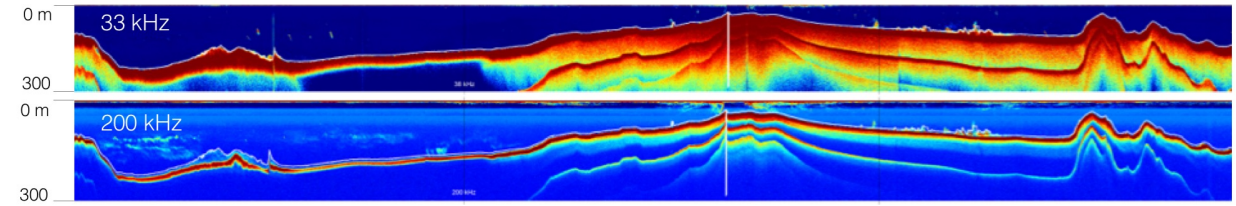

Figure S10. Example of a seafloor correction output. Top row is 33 kHz output, bottom row is 200 kHz. Color palette is same as that used in Hydrobox echogram display software. The "fixed" seafloor is superimposed on the transect's georectified echogram. Obvious imperfections remain, hence the next step of manual seafloor correction.

Manual seafloor correction

The automated seafloor correction process is imperfect. For those pings where the "fixed" seafloor is still obviously erroneous (evidenced by the echogram of the corrected seafloor), the NOAA data were used as the best estimate of local depth. If there is no NOAA data within 0.005 degrees of the ping, the depth has to be updated to “NA”.

A JPEG of the echogram with automatic seafloor correction is reviewed in ImageJ, in which EMK drew rectangles around erroneous segments of seafloor and save those rectangle's measurements to a .CSV. Those measurements correspond to the start and end rows of problematic stretches of seafloor in the echo .CSV files. The conversion from JPEG pixel measurements to dataframe coordinates is not perfect due to margins that scale along with the length of the echo file, so a conversion routine was developed in R. To do so EMK manually converted measurements from 39 echogram JPEG's from 2014 echodata to the coordinates in their corresponding .CSV. Based on these manual conversions a linear model was defined that enabled EMK to automate the conversion. For each JPEG, the problematic segments of seafloor are isolated and replaced with GPS-matched CHS bathymetric data. New .CSVs, echograms, and seafloor correction plots are saved to file.

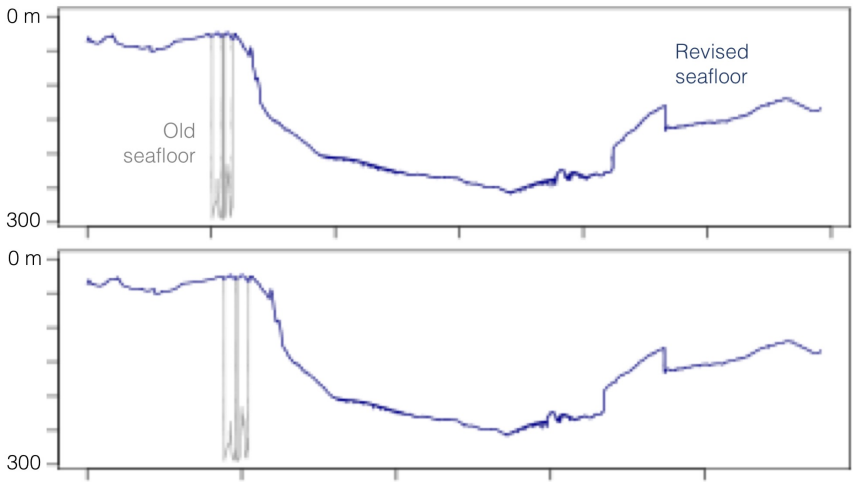

Figure S11. Results of manual seafloor correction. Dark gray is the auto-corrected seafloor, blue is the seafloor after manual correction. Top row is 33kHz readings, bottom row is 200kHz.

Manual noise removal

Each day’s backscatter were then visually reviewed for manual removal of regions of noise caused by engine cavitation, depth sounders from passing vessels, tracks of diving whales, and kelp. EMK reviewed each JPEG in ImageJ, drew rectangles around noise, saved those measurements to a text file, then ran a script in R that replaces that noisy data with NA values in the corresponding .CSV.

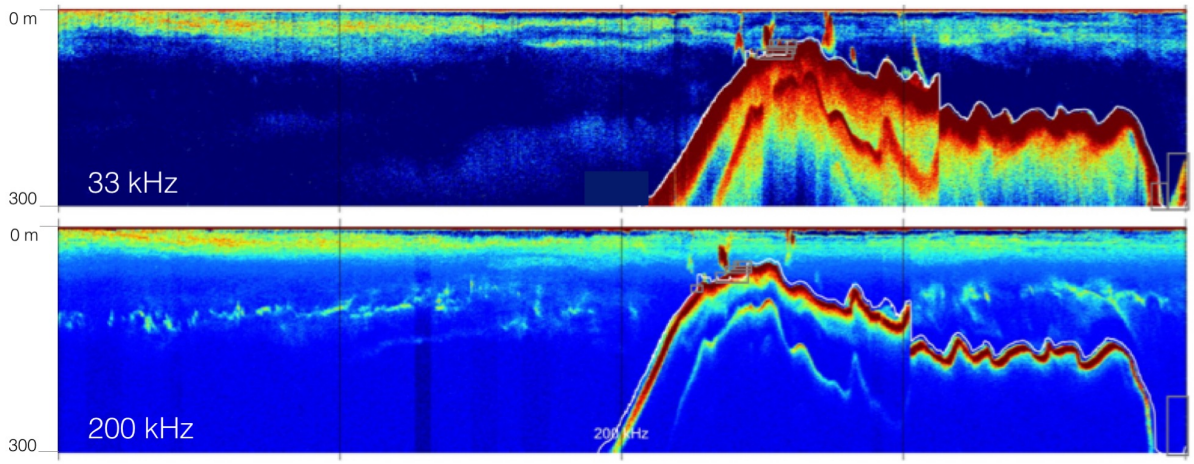

Figure S12. Record of manual selections (grey boxes), made in ImageJ, of "bad areas" in Campania transect (2 June 2015). Top row is 33 kHz output, bottom row is 200 kHz. Color palette is same as that used in Hydrobox echogram display software.

```
7,5,0,0,1,0,0,0,0,0,1,0,0,0,0,0,0,0,0,0,0,0,0,0,0,0,1,0,0
,0,0,0,0,0,0,32,0,0,0,0,0,1,136,0,0,16,0,0,0,0,0,0,0,1,0,0,
,0,16,16,0,0,0,0,52,0,0,0,0,64,0,0,0,0,0,0,0,0,0,0,0,0,NA,N
0,0,0,0,0,0,0,0,0,0,0,0,0,0,0,0,0,0,1,0,0,0,0,0,18,0,0,0,0,0,
,0,0,0,0,0,0,0,0,0,0,0,0,0,0,0,0,0,0,0,0,0,0,0,0,0,0,0,0,0,NA
,0,0,0,0,0,0,0,0,1,0,0,0,0,0,0,0,16,34,0,0,0,0,0,0,0,0,0,0,0,0,
,0,0,0,0,0,0,0,0,0,0,0,0,0,0,0,1,0,0,32,0,0,0,112,0,0,0,65,114,56
0,0,0,0,0,0,0,0,0,0,32,0,0,0,0,0,0,2,0,0,0,1,0,0,0,0,0,0,0,0,0,11
,0,0,0,0,0,0,0,0,0,0,0,0,0,0,0,0,0,0,3,0,0,0,16,0,0,0,0,0,0,99,156,16
,0,3,0,16,0,0,0,0,0,0,0,0,49,0,0,0,0,0,2,48,0,0,0,0,0,0,0,0,0,0
0,100,89,0,3,0,0,1,2,83,85,0,0,0,0,0,16,0,0,0,0,0,0,0,0,0,71,
0,48,3,0,0,0,0,0,0,0,0,0,64,18,64,115,49,0,0,0,0,0,0,0,NA,NA,
,0,0,0,0,0,0,1,0,NA,NA,NA,NA,NA,NA,NA,NA,NA,NA,NA,NA,NA,NA,NA,NA,NA
,0,0,0,0,0,0,0,0,0,NA,NA,NA,NA,NA,NA,NA,NA,NA,NA,NA,NA,NA,NA,NA,NA,
0,0,0,48,22,0,0,0,0,0,2,16,NA,NA,NA,NA,NA,NA,NA,NA,NA,NA,NA,NA,N
1,2,48,3,NA,NA,NA,NA,NA,NA,NA,NA,NA,NA,NA,NA,NA,NA,NA,NA,NA,NA,NA
34,35,0,0,0,0,0,0,0,64,NA,NA,NA,NA,NA,NA,NA,NA,NA,NA,NA,NA,NA,NA
17,0,0,0,0,0,0,0,0,0,0,0,0,0,0,0,NA,NA,NA,NA,NA,NA,NA,NA,NA,NA,N
,39,16,16,0,0,0,0,0,0,0,64,0,0,65,0,0,0,NA,NA,NA,NA,NA,NA,NA,
0,0,0,0,0,0,0,0,0,0,0,0,0,NA,NA,NA,NA,NA,NA,NA,NA,NA,NA,NA,NA,
0,0,0,48,37,0,0,0,0,0,0,NA,NA,NA,NA,NA,NA,NA,NA,NA,NA,NA,NA,NA,N
0,0,0,0,0,0,0,0,0,0,0,0,0,NA,NA,NA,NA,NA,NA,NA,NA,NA,NA,NA,NA,N
0,0,0,0,0,0,0,0,0,0,0,0,0,NA,NA,NA,NA,NA,NA,NA,NA,NA,NA,NA,NA,
```

Figure S13. Result of manual filtration, in which “bad areas” are replaced with “NA” entries.

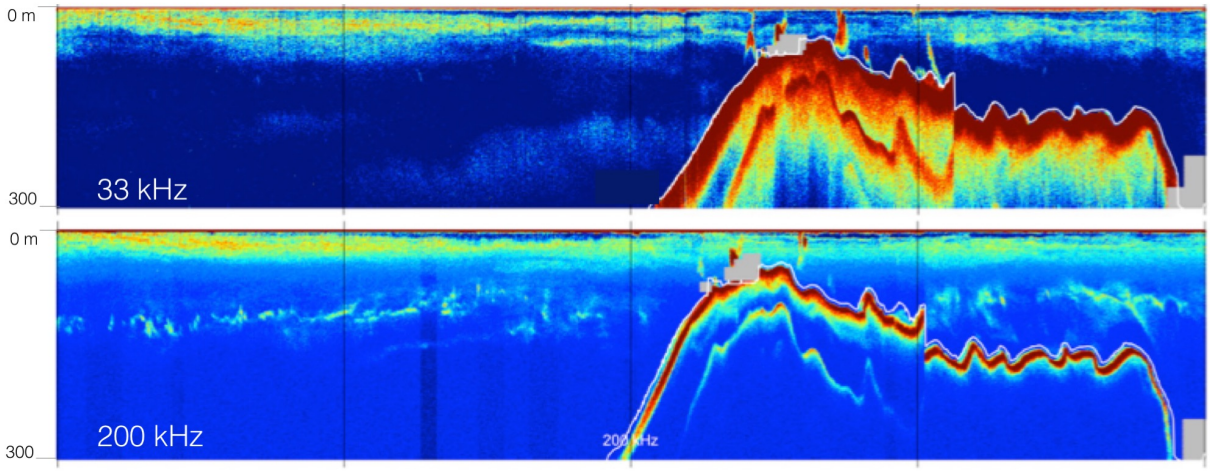

Figure S14. Result of manual filtration on Campania transect (2 June 2015). Top row is 33 kHz output, bottom row is 200 kHz. Color palette is same as that used in Hydrobox echogram display software.

Noise floor filter

Next, weak backscatter whose intensity registers below a background noise floor are removed using a filter. Values below this floor are assumed to be noise, values above are considered biological and potentially qualify as whale prey. Based on visual examination of multi-season echograms, noise floors are set to pixel values of 135 and 125 for 33kHz and 200kHz backscatter, respectively.

In this step, surface and seafloor buffers are also applied, in which the top 6m of the water column are removed as well as the 6m of backscatter above the seafloor.

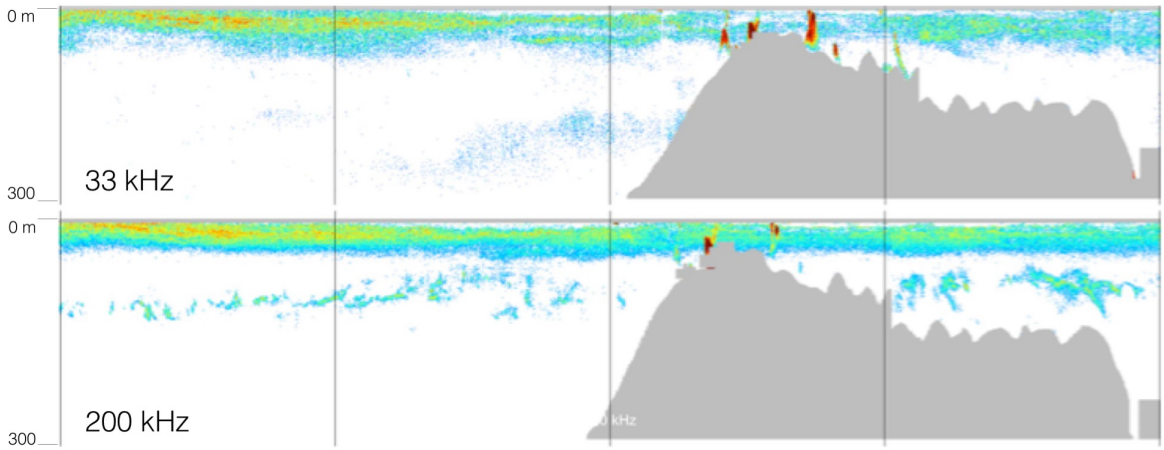

Figure S15. Backscatter after application of biological noise floor. White areas are backscatter that did not register above noise floor threshold. Grey areas are seafloor or manually removed noise. Color palette for "biological" backscatter is same as that used in Hydrobox echogram display software. Top row is 33 kHz output, bottom row is 200 kHz.

FINALIZE DATASETS

Package into transect blocks

On rare occasions, transect effort within a single waterway had to span more than one day due to inclement weather. Such days were concatenated into a single file so that effort in each waterway during a sampling period was represented by a single file. Also, data in each file were sequenced to progress from south to north. To make sure that the transect was packaged correctly, annotated maps of each packaged file were produced.

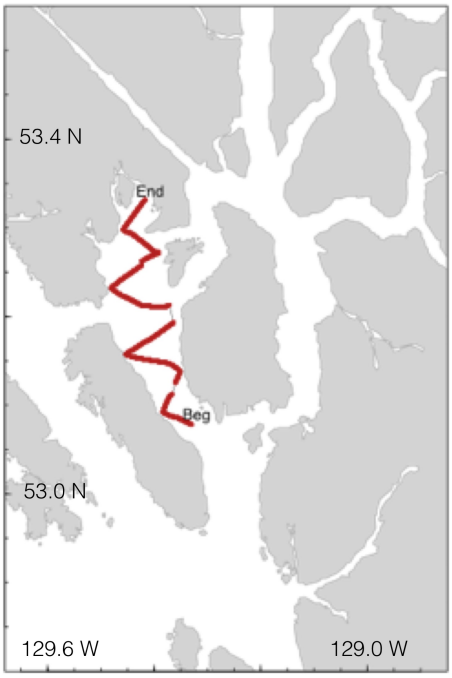

Figure S16. Example of annotated map of transect trackline based on echosounder data (from 30 May 2015).

Echogram visualization scheme

To simplify visualizations of echodata and verify subsequent scrutinization procedures, echograms were created in which the two frequencies are overlaid. The colors for each frequency are graded monochromatically and made translucent, so that areas of overlap can be seen. The width of the JPEG was set to a standard 5:1 ratio.

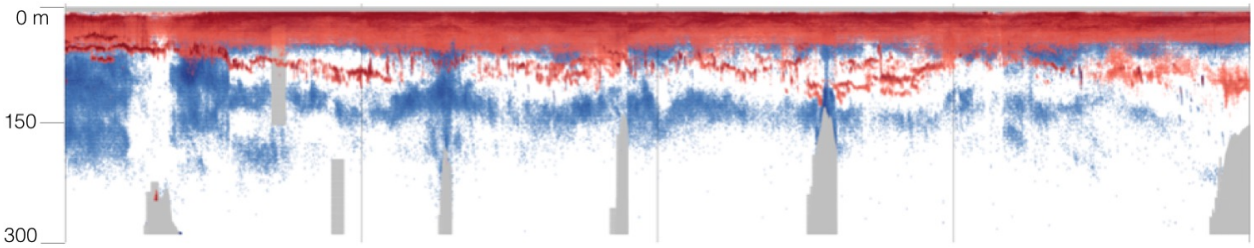

Figure S17. A combined echogram from 30 May 2015 in Squally channel, with the two frequencies overlayed with translucency (blue = low frequency, red = high frequency).

Scrutinization: prey patch filtration

In order to reduce each backscatter frequency further to display only patches that are probable whale prey, semi-automatic filters were applied based on patch characteristics so that, to the extent possible, 33kHz backscatter represents only small schooling fish while 200kHz backscatter represents euphausiids. Filter parameters were adjusted broadly for each month, and, in the case of anomalous noise levels, each day. This step was necessary because the biological noise floor threshold may have missed strongly backscattering water features such as particulate debris, inordinately dense mats of phytoplankton, and strong haloclines, all of which can be prominent within this fjord system. Moreover, each frequency

reflects organisms that were not likely whale prey (e.g., fry and siphonophores at 33 kHz and copepods at 200 kHz; Macaulay et al. 1995, Barraclough et al. 1969).

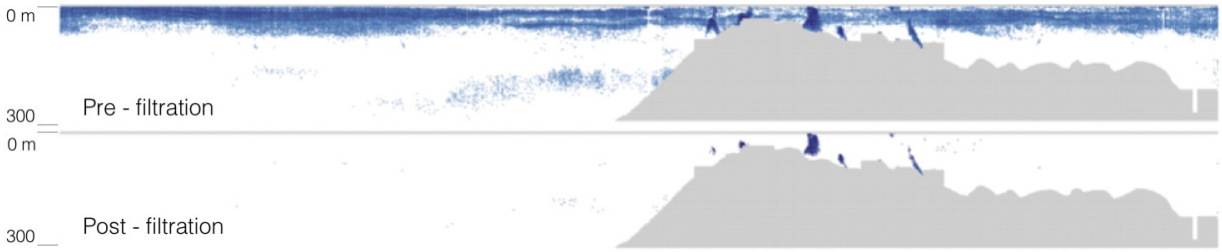

Figure S18. 33kHz backscatter, before (top) and after (bottom) prey patch filtration. From 2 June 2015 in Campania Sound.

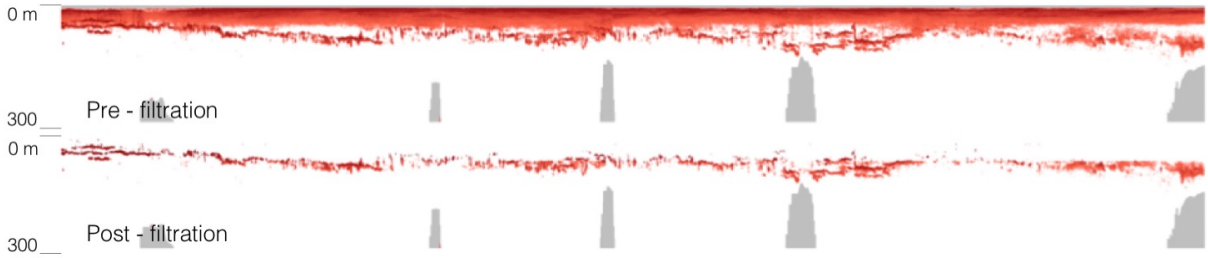

Figure S19. 200kHz backscatter, before (top) and after (bottom) prey patch filtration. From 30 May 2015 in Squally Channel.

Because air-bladdered fish can induce backscatter on both 33kHz and 200kHz frequencies (Foote 1980, Coyle and Cooney 1992, Kang et al., 2002, Jech et al., 2006), a simplified version of "frequency-differencing" was then implemented, in which 200 kHz backscatter that overlapped with 33 kHz was removed.

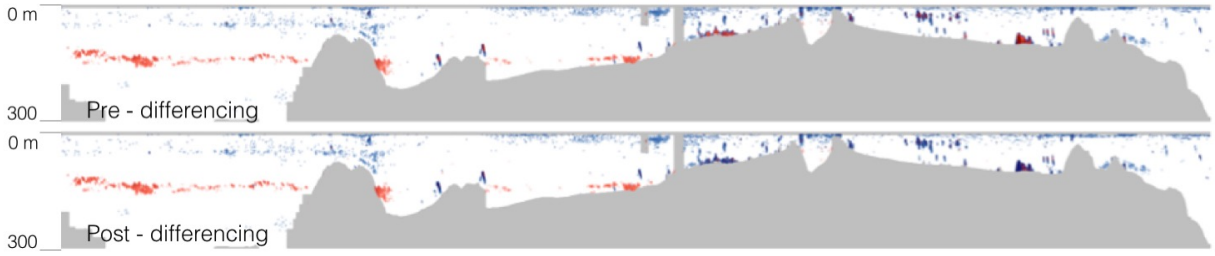

Figure S20. Before (top) and after (bottom) frequency differencing. From 18 July 2015 in Verney Pass.

The figures that follow provide examples of finalized acoustic datasets, first for focal follows (Fig. S21), then for each sampling period in 2015 (Figs. S22 – S27).

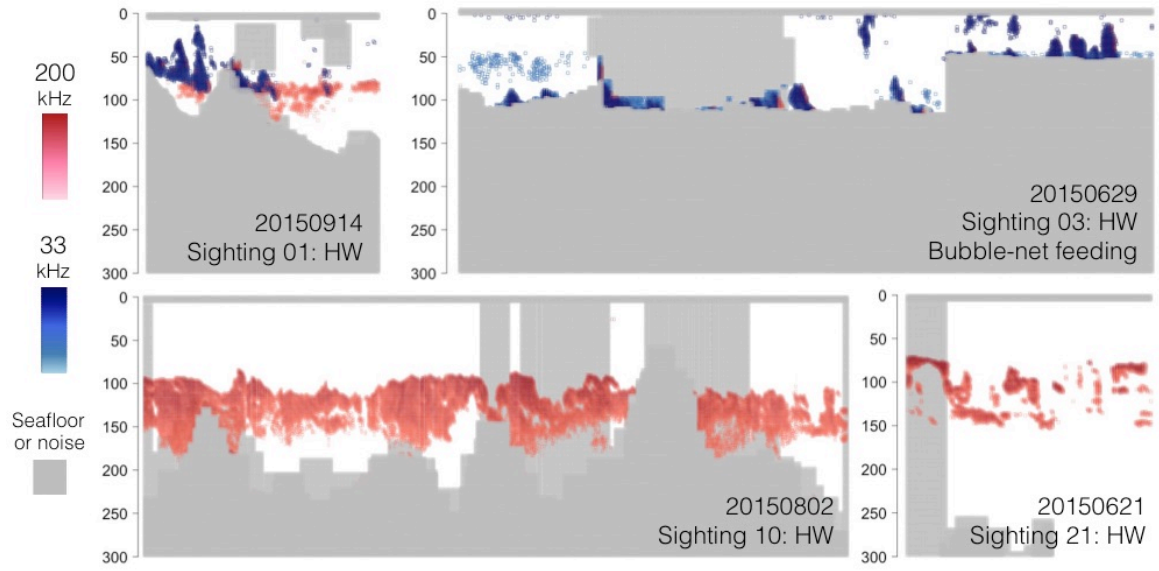

Figure S21. Examples of acoustic backscatter collected during focal follows. Each pane is a separate focal follow, designated with its date, sighting number, species (HW=humpback), and uncommon behaviors, if any. Top row: focal follows containing backscatter that is likely attributable to small schooling fish; the top left focal follow is an example of both fish- and euphausiid-like backscatter occurring in close proximity. Bottom row: Focal follows with backscatter attributable to euphausiids only. Y-axis is depth (m), X-axis is chronological order of echosounder pings geo-rectified into 10m horizontal bins, and backscatter is represented in color gradients representing backscatter intensity (red = 200 kHz, blue = 33 kHz, grey = seafloor or manually removed self-noise).

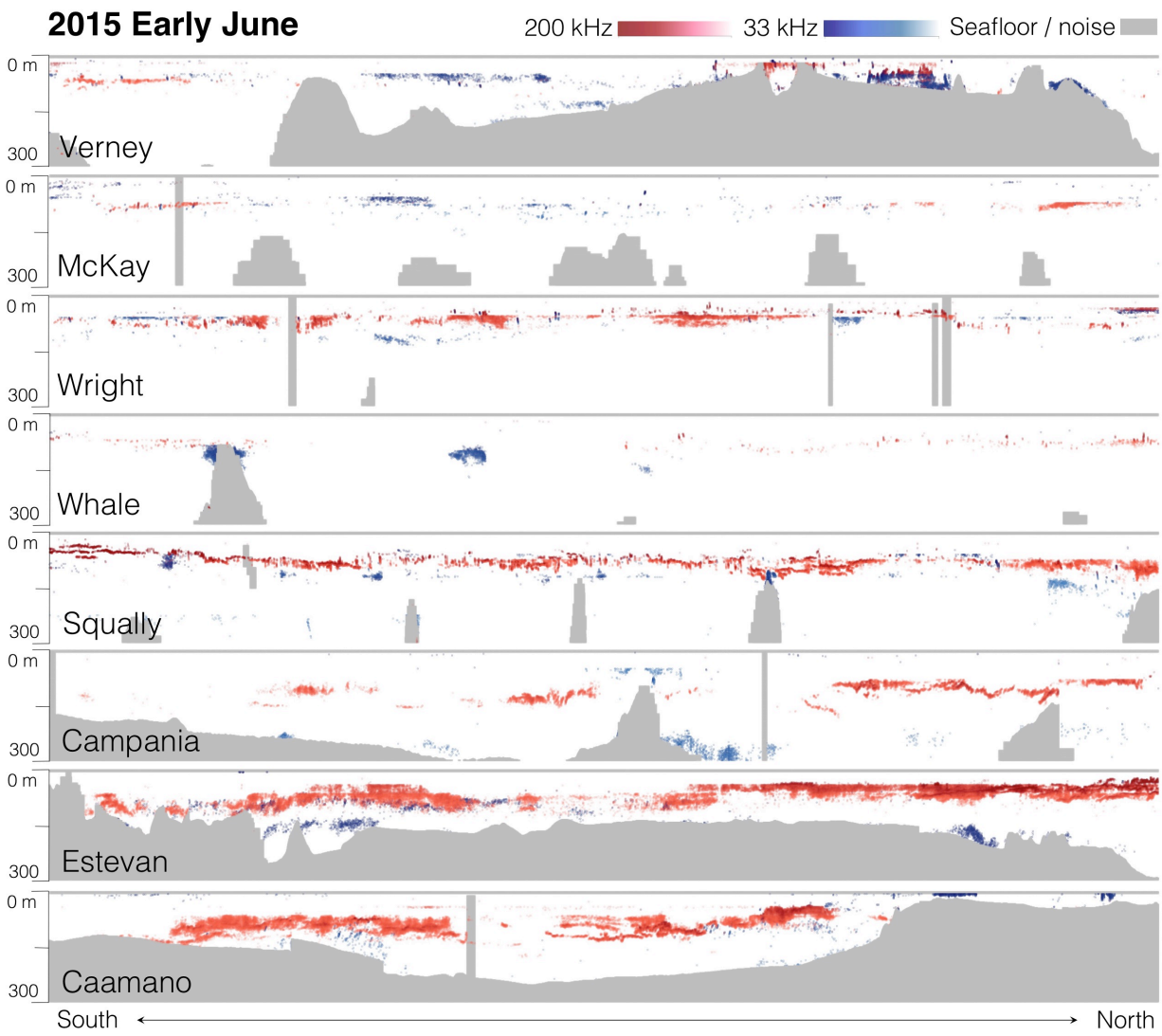

Figure S22. Profiles of acoustic backscatter from early June 2015. Each row displays transects within a single channel of the Kitimat Fjord System, from south (left) to north (right), and from sea surface (top of row) to 300m depth (bottom of row). Channels are arranged from offshore (bottom) to inshore (top). Prey-like backscatter is presented in two color-scales: red scale = 200 kHz backscatter filtered to euphausiid-like patches, blue scale = 33 kHz filtered to schooling fish-like patches, grey = seafloor.

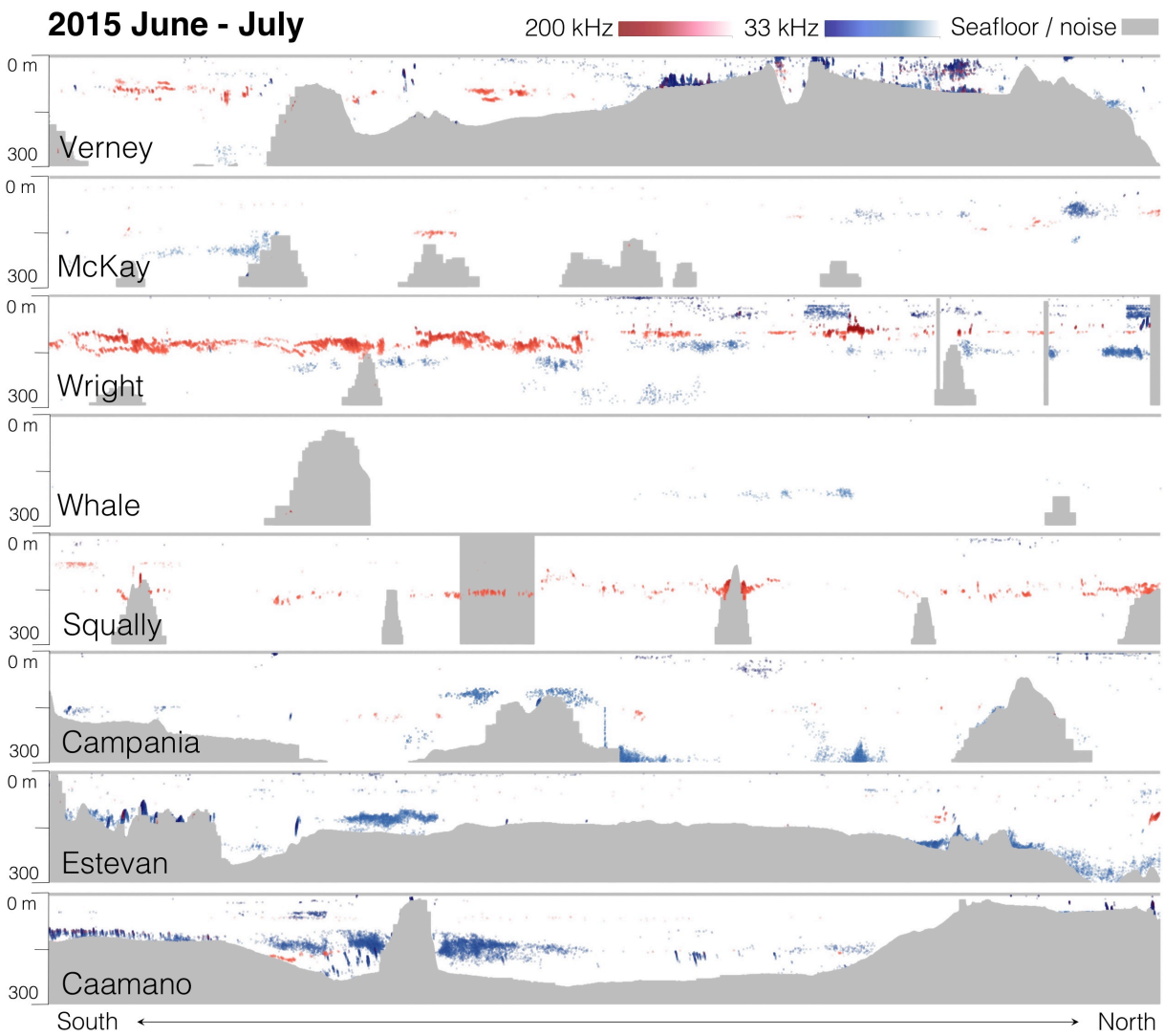

Figure S23. Profiles of acoustic backscatter from late June to early July 2015. Each row displays transects within a single channel of the Kitimat Fjord System, from south (left) to north (right), and from sea surface (top of row) to 300m depth (bottom of row). Channels are arranged from offshore (bottom) to inshore (top). Prey-like backscatter is presented in two color-scales: red scale = 200 kHz backscatter filtered to euphausiid-like patches, blue scale = 33 kHz filtered to schooling fish-like patches, grey = seafloor.

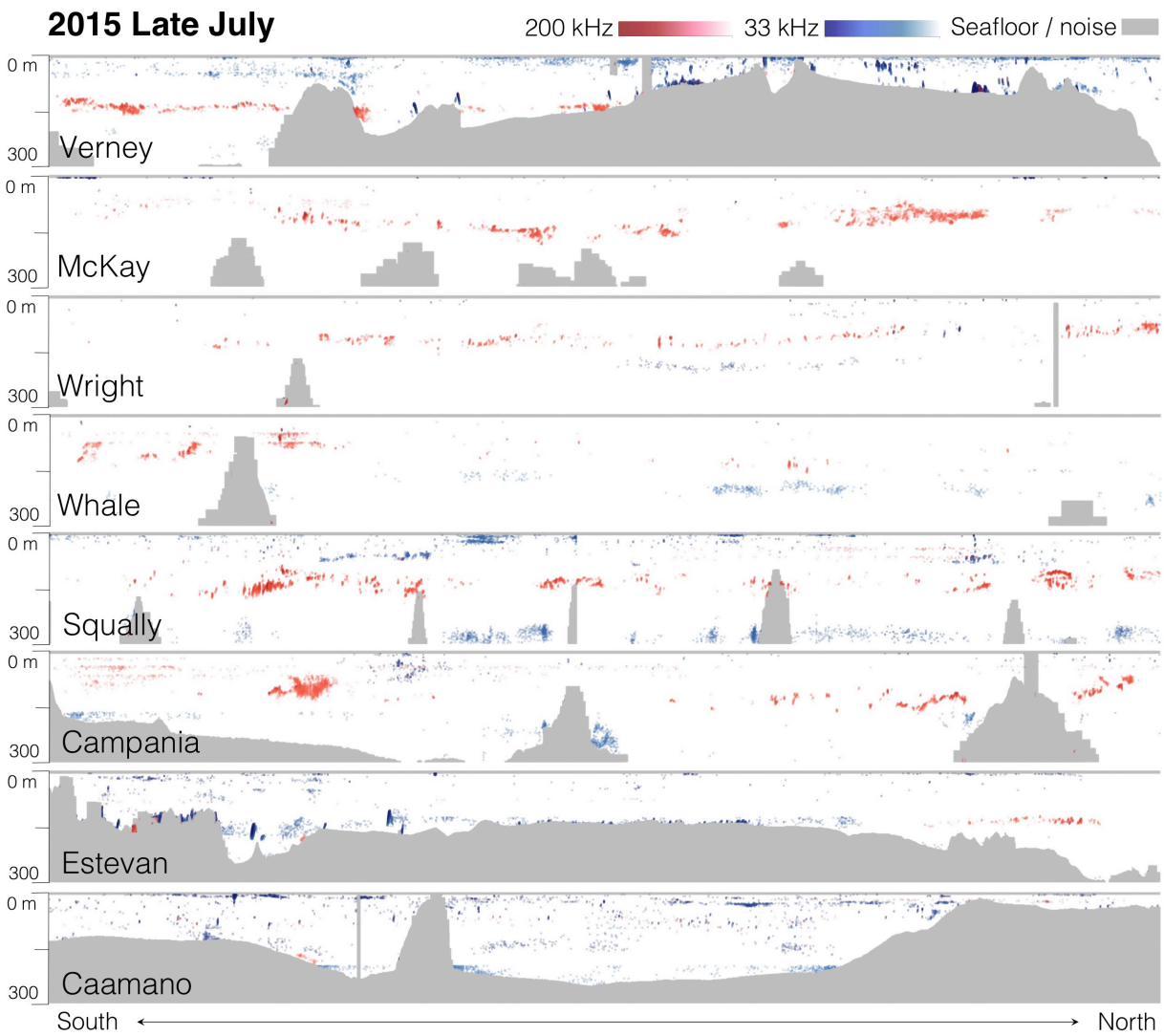

Figure S24. Profiles of acoustic backscatter from late July 2015. Each row displays transects within a single channel of the Kitimat Fjord System, from south (left) to north (right), and from sea surface (top of row) to 300m depth (bottom of row). Channels are arranged from offshore (bottom) to inshore (top). Prey-like backscatter is presented in two color-scales: red scale = 200 kHz backscatter filtered to euphausiid-like patches, blue scale = 33 kHz filtered to schooling fish-like patches, grey = seafloor.

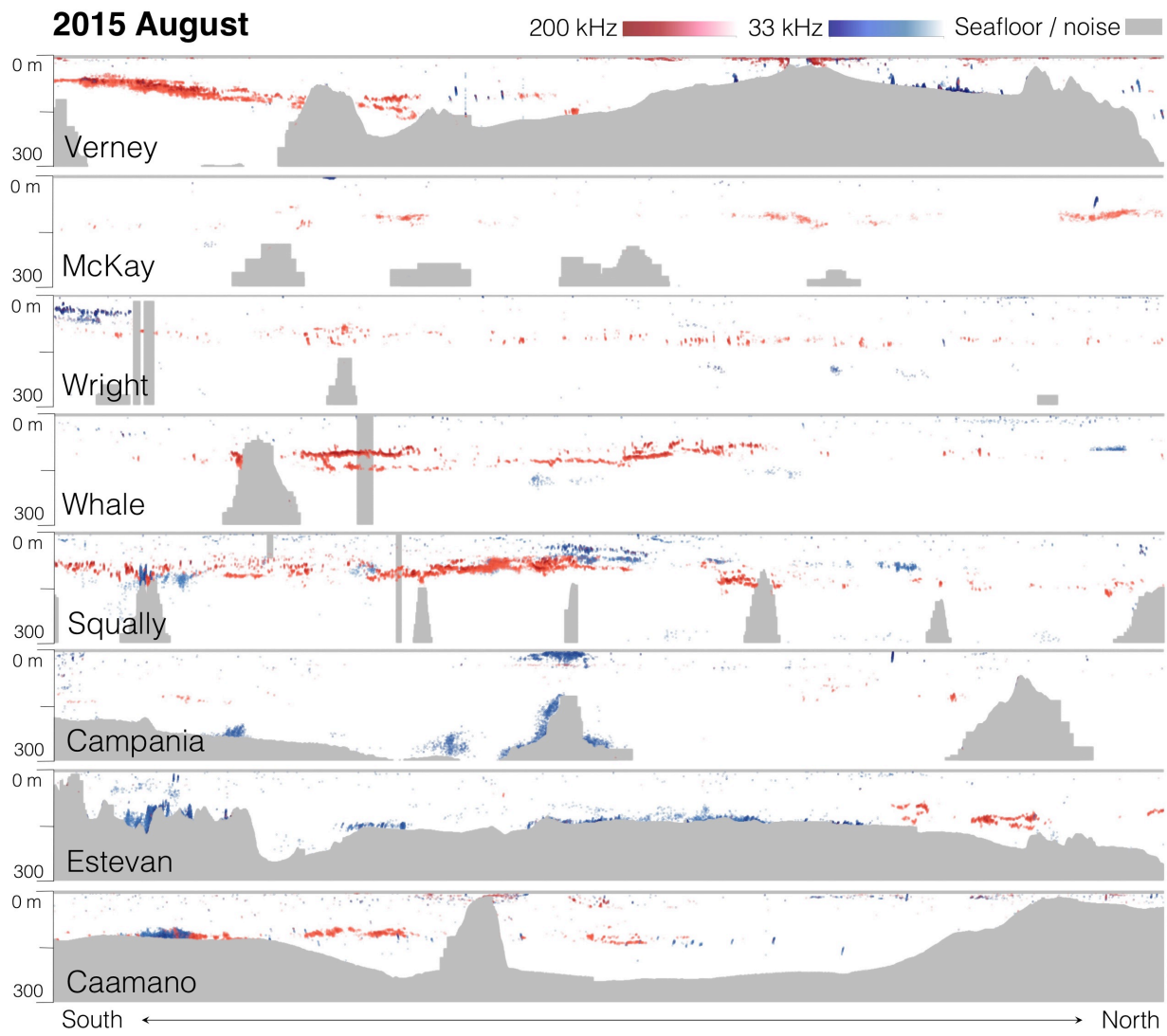

Figure S25. Profiles of acoustic backscatter from August 2015. Each row displays transects within a single channel of the Kitimat Fjord System, from south (left) to north (right), and from sea surface (top of row) to 300m depth (bottom of row). Channels are arranged from offshore (bottom) to inshore (top). Prey-like backscatter is presented in two color-scales: red scale = 200 kHz backscatter filtered to euphausiid-like patches, blue scale = 33 kHz filtered to schooling fish-like patches, grey = seafloor.

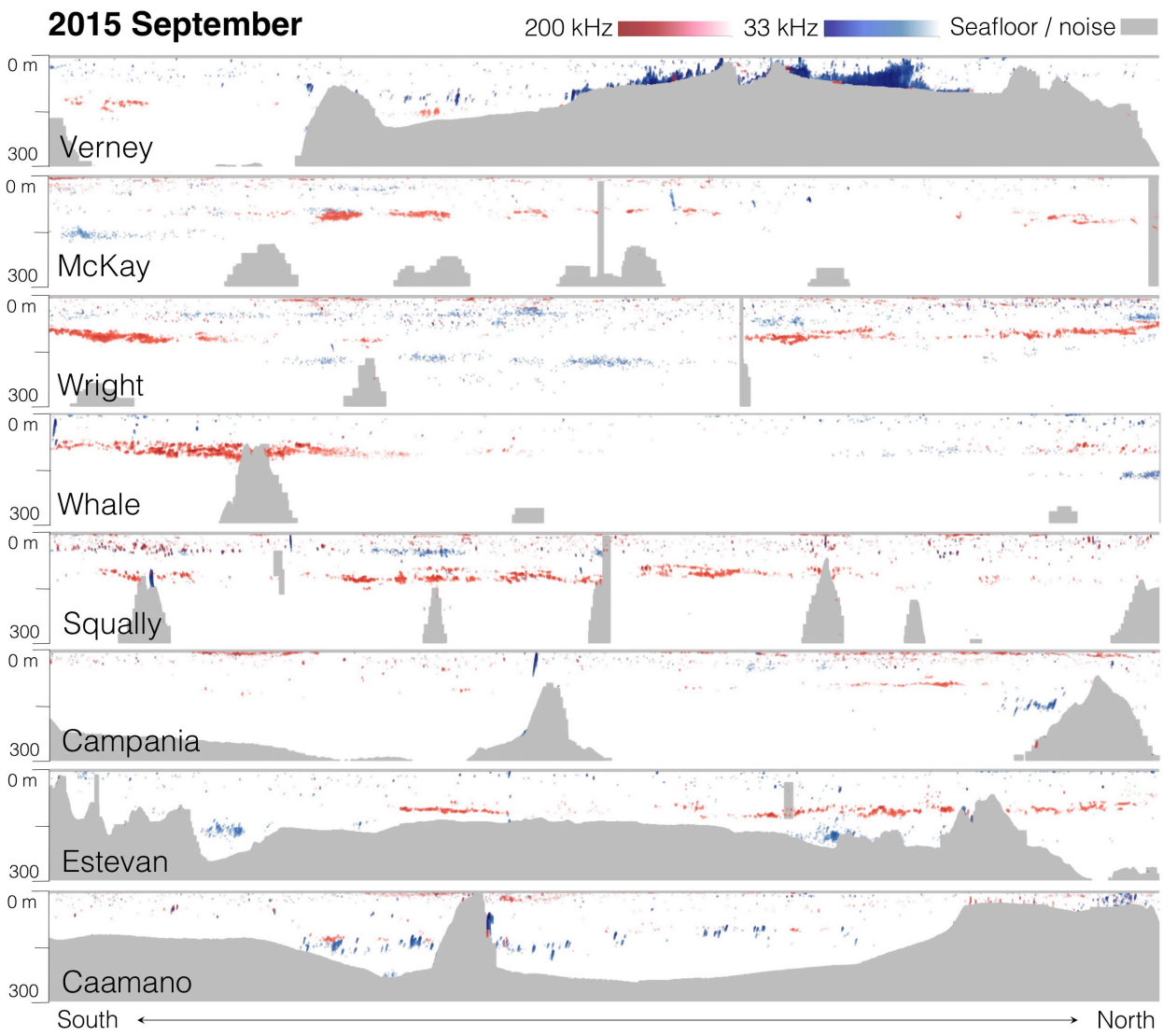

Figure S26. Profiles of acoustic backscatter from September 2015. Each row displays transects within a single channel of the Kitimat Fjord System, from south (left) to north (right), and from sea surface (top of row) to 300m depth (bottom of row). Channels are arranged from offshore (bottom) to inshore (top). Prey-like backscatter is presented in two color-scales: red scale = 200 kHz backscatter filtered to euphausiid-like patches, blue scale = 33 kHz filtered to schooling fish-like patches, grey = seafloor.

BACKSCATTER METRICS

Middle-priced echosounders like that used in this study can characterize prey-like backscatter but cannot quantify the biomass of constituent taxa. We developed 4 simple metrics for each filtered frequency, described below and depicted in Fig. S27.

1. **Total backscatter (T):** The mean sum of pixel values of prey-like backscatter; this is a proxy for the quantity of potential prey available.
2. **Backscatter intensity (I):** The mean pixel value of prey-like backscatter; this is a proxy that can represent the density, body size, and/or swarm characteristics of potential prey swarms.
3. **Mean depth (Z):** The mean of the depth distribution of prey-like backscatter. This metric was not used in the present paper but we include it here nonetheless as a candidate that we considered.
4. **Vertical dispersion (D):** The standard deviation of the depth distribution of prey-like backscatter; this is a proxy for the vertical extent of prey swarms; highly dispersed backscatter may be less ideal for batch-feeding predators such as rorqual whales.

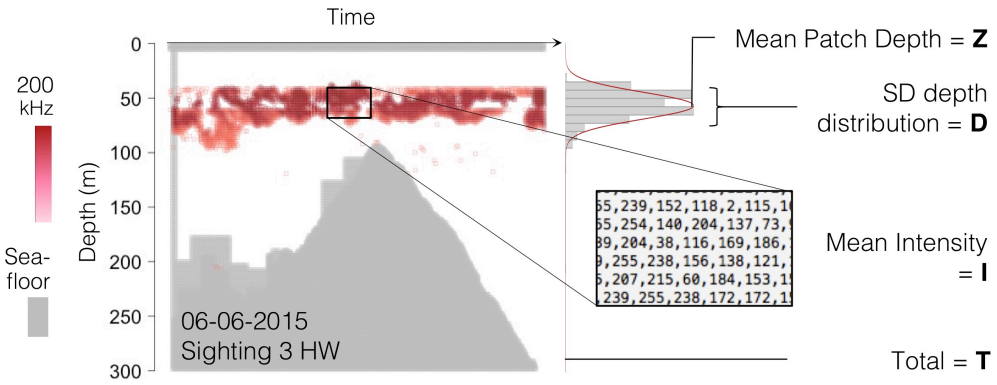

Figure S27. Depiction of backscatter metrics, explained in text above. Y-axis is depth (m), X-axis is chronological order of echosounder pings geo-rectified into 10m horizontal bins, and backscatter is displayed on a red color gradient (deeper red = higher backscatter return; grey = seafloor or manually removed self-noise). Backscatter is stored at rows (pings) of 200 columns of pixel values (each pixel representing backscatter within a 1.5m vertical bin; box inset). Example shown is from a focal follow of a humpback (Sighting 03 on 6 June 2015).

These metrics were cross-checked pairwise for collinearity. Figure 8 in the main paper displays interpolated maps for total backscatter, while Figure S28 below displays interpolated maps for 200 kHz backscatter intensity and vertical dispersion:

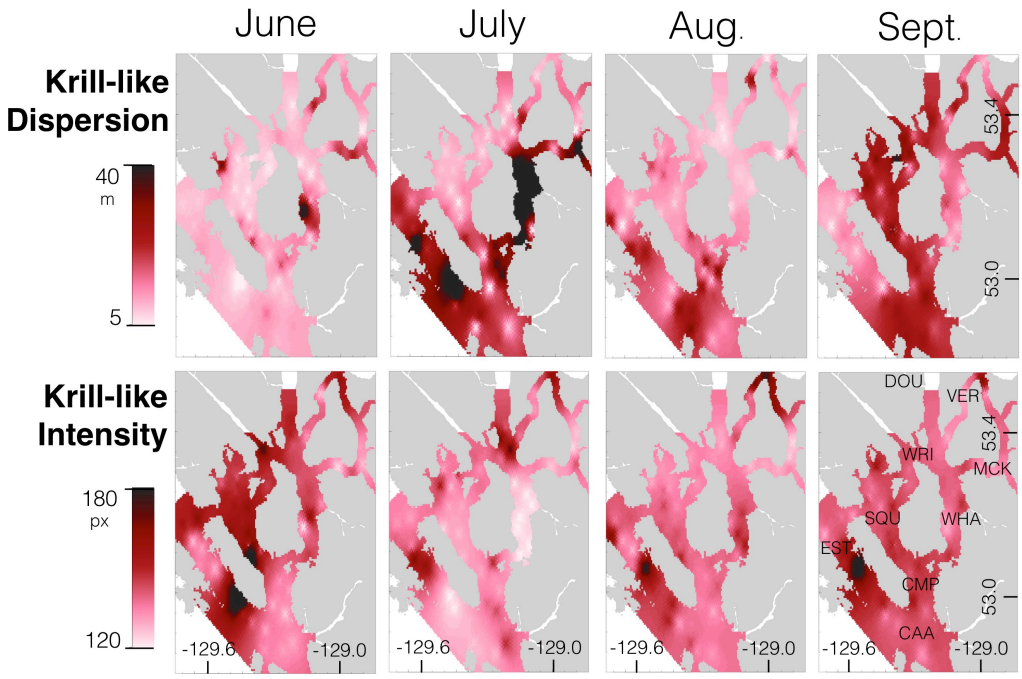

Figure S28. Maps of the dispersion and intensity of krill-like backscatter (filtered 200 kHz) interpolated from 5km bins of trackline within each monthly survey, summer 2015. Color scales range from noise floor to the season's maximum reading. Interpolation was performed using inverse path weighted distance, a function that linearly weights combinations of sampled points based on their distance from the interpolation cell, accounting for land obstruction.

VERIFICATION

To visually ground-truth the objects causing krill-like backscatter on echograms, we developed the Krill Imaging and Scrambling System (KISS), a weight-balanced deepwater imaging towfish apparatus with mounted Go-Pro and 2,000-lumen LED spotlight in pressure-rated housing (Group B Inc.). KISS casts were conducted regularly throughout the season in various backscatter conditions. The KISS was deployed on 250 meters of line marked every 25m so that KISS depth could be recorded throughout a cast. Recorded video was retrieved and frames were assigned depths using timestamp matching with data entry software output. By comparing recorded video to backscatter collected during the cast, we were able to confirm that our processed 200 kHz backscatter represented swarming euphausiids (example in Fig. S29)

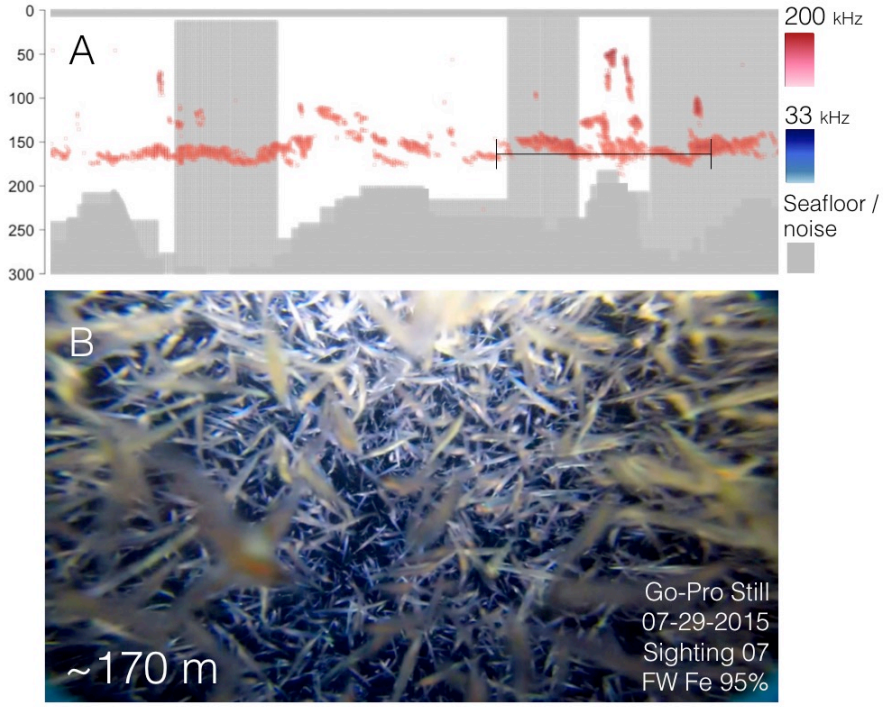

Figure S29. Below: A) Acoustic backscatter collected during a focal follow of 3 fin whales on 29 July 2015. Y-axis is depth (m), X-axis is chronological order of echosounder pings geo-rectified into 6m horizontal bins. Greyed-out sections are periods of high engine RPM that compromised 33 kHz readings and were manually removed. B) Still-frame of Go-Pro video taken during same focal follow using the Bangarang Krill Imaging and Scrambling System (KISS), displaying dense aggregations of euphausiids at approximately 170m. Black bracketed line in panel A displays the time window in which KISS cast descended from 150m to 200m. Full video at: http://www.rvbangarang.wordpress.com/moments

Zooplankton tows

Three daytime, plummet-style zooplankton tows (333u, 0.7m diameter, OAR 6:1, dropped to 250m seafloor permitting; designed according to Keen 2015) were taken at the stations within each channel. A plummet net is a down-fishing zooplankton sampler that has no mouth obstructions and is cinched shut when the desired depth is reached (Heron 1982). Samples were immediately preserved in 5% formaldehyde-seawater solution.

Figure S30. Photograph of a 2015 zooplankton sample; black dots are the eyes of euphausiids.

Acoustic backscatter was recorded during work at oceanographic stations, affording the opportunity to ground-truth our backscatter processing routine. Noise and patch filtration steps were conducted with the same parameterization and scrutiny described above, the only difference being that station data were subset to only the pings recorded during the net's descent (sampling) phase. Backscatter caused by the net (e.g., Fig. S31) was manually removed as well. Backscatter metrics were then calculated. Euphausiid individuals in each sample were counted by collaborators at Oregon State University (Katie Qualls, Bernard lab, pers. comm.). The numbers of other major zooplankton taxa were also approximated, including copepods, amphipods, chaetognaths, and other gelatinous taxa. Krill counts were found to be correlated with our total 200 kHz backscatter metric ($n = 40$, $p = 0.006$, $r^2 = 0.18$; Fig. S32), while other taxa were not correlated (copepods: $p = 0.81$; amphipods: $p = 0.895$; chaetognaths: $p = 0.50$; other gelatinous: $p = 0.298$). This verified the sufficiency of our backscatter processing techniques for our purposes here.

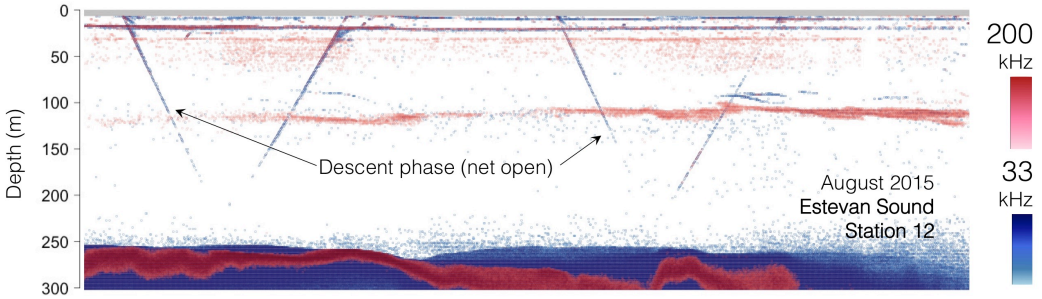

Figure S31. Two zooplankton tows at an oceanographic station in August 2015. Backscatter is presented in two color-scales: red scale = 200 kHz backscatter, blue scale = 33 kHz.

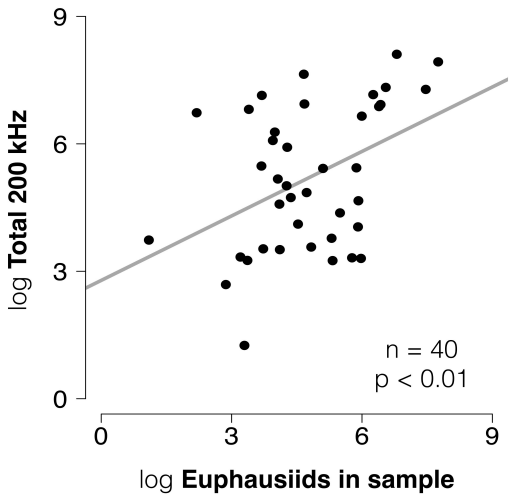

Figure S32. Correlation ($r^2 = 0.18$) between euphausiids sampled at oceanographic stations and filtered acoustic backscatter (Total 200 kHz metric) recorded during zooplankton tows.

LITERATURE CITED

Andersen, N. R., and B. J. Zahuranec (eds.), 1977. Oceanic Sound Scattering Prediction. Plenum Press, New York: 859 pp

Bary BM. 1966. Backscattering at 12 kc/s in relation to biomass and numbers of zooplanktonic organisms in Saanich Inlet, British Columbia. Deep-Sea Res 13: 655–666

Barraclough, WE, Lebrasseur, RJ and RO Kennedy. 1969. Shallow scattering layer in the sub-Arctic Pacific Ocean. Detection by high frequency echo sounder. Science 166:611–613

Benoit-Bird, KJ, WL Au, RE Brainard, MO Lammers. 2001. Diel horizontal migration of the Hawaiian mesopelagic boundary community observed acoustically. 217:1–14

Benoit-Bird, KJ & WWL Au. 2003. Prey dynamics affect foraging by a pelagic predator (Stenella longirostris) over a range of spatial and temporal scales. Behavioral Ecology and Sociobiology 53(6):364–373

Burger, AE, JF Piatt. 1990. Flexible time budgets in breeding Common Murres: buffers against variable prey availability. Stud. Avian Bio. 14:71–83

Cochrane, N. A., Sameoto, D. D., and Herman, A. W. 2000. Scotian Shelf euphausiids and silver hake population changes during 1984-1996 measured by multi-frequency acoustics. - ICES Journal of Marine Science, 57: 122–132

Coyle, KO and RT Cooney. 1992. Water column sound scattering and hydrography around the Pribilof Islands, Bering Sea

Dolphin, WF. 1988. Foraging dive patterns of humpback whales, Megaptera novaeangliae, in southeast Alaska: a cost-benefit analysis. Can. J. Zool. 66: 2432–2441

Farquhar, G. B. (ed.), 1971. Proceedings of an International Symposium on Biological Sound Scattering in the Ocean, Maury Center for Ocean Science, Washington, D. C.: 629 pp

Foote, K.G. (1980) Importance of the swimbladder in acoustic scattering by fish: a comparison of gadoid and mackerel target strengths. J. Acoust. Soc. Am. 67, 2084–9

Heron, A.C. 1982. A vertical free fall plankton net with no mouth obstructions. Limnology and Oceanography 27(3):380–383

Jech, J Michael and WL Michaels. 2006. A multifrequency method to classify and evaluate fisheries acoustics data. Can. J. Fish. Aquat. Sci. 63:2225–2235

Kang, M, M. Furusawa, and K Miyashita. 2002. Effective and accurate use of difference in mean volume backscattering strength to identify fish and plankton. ICES Journal of Marine Science 59:794-804

Keen, EM. 2015. Net savvy: a practical guide to zooplankton sampler design. NOAA-TM-NMFS-SWFSC-545

Macaulay, MC, KF Wishner, KL Daly. 1995. Acoustic scattering from zooplankton and micronekton in relation to a whale feeding site near Georges Bank and Cape Copd. Continental Shelf Research 15(4/5):509–537

MacLennan, D.N., Fernandes, P.G. & Dalen, J. (2002). A consistent approach to definitions and symbols in fisheries acoustics. ICES Journal of Marine Science: Journal du Conseil, 59, 365

NOAA. 2013. British Columbia 3 arc-second bathymetric digital elevation model. Version 1. National Center for Environmental Information. www.ngdc.noaa.gov

O'Driscoll, R. 1998. Description of spatial pattern in seabird distributions along line transects using neighbor K statistics. 165:81–94

Piatt, JF. 1987. The behavioural ecology of common murre and Atlantic puffin predation on capelin: implications for population biology. PhD, Memorial Univ. of Nefoundland, St. John's

Piatt, JF.1990. The aggregative response of Common Murres and Atlantic Puffins to schools of capelin. Stud. Avian Bio. 14:36–51

Piatt, JF and DA Methven. 1992. Threshold foraging behavior of baleen whales. Marine Ecology Progress Series 84:205–210

R Core Team (2013) R: A language and environment for statistical computing. R Foundation for Statistical Computing, Vienna, Austria. URL http://www.R-project.org/

Romaine, SJ, DL Mackas, and MC MacAulay. 2002. Comparison of euphausiids population size estimates obtained using replicated acoustic surveys of coastal inlets and block average vs. geostatistical spatial interpolation methods. Fisheries Oceanography 11:2, 102–115

Rowe, DK. 1993. Identification of fish responsible for five layers of echoes recorded by high-frequency (200kHz) echosounding in Lake Rotoiti, north Island, New Zealand. New Zealand Journal of Marine and Freshwater Research

Sato, M., JF Dower, E Kunze, R Dewey. 2013. Second-order seasonal variability in diel vertical migration timing of euphausiids in a costal inlet. Marine Ecology Progress Series. Vol. 480: 39–56

Stanton, TK, D Chu, and PH Wiebe. 1996. ICES Journal of Marine Science. 53:289–295

Wiebe, P.H., Stanton, T.K., Benfield, M.C., Mountain, D., Greene, C.H., 1997. High-frequency acoustic volume backscattering in the Georges Bank coastal region and its interpretation using scattering models. Institute of Electrical and Electronic Engineers Journal of Oceanic Engineering 22, 445–464

Yule, DL. 2000. Comparison of horizontal acoustic and purse-sein esitmates of salmonid densities and sizes in eleven Wyoming Waters. North American Journal of Fisheries Management 20:3, 759–775